Electrokinetic Dispersion in Capillary Electrophoresis

A "Taylor" dispersion-type model is developed for the electrokinetic dispersion coefficient of a solute in capillary electrophoresis that accounts for the effects of Poiseuille and/or electro-osmotic flow of the elutant for the case of low ζ potential. The expression obtained for the height equivalent of a theoretical plate is compared with experimental results reported in the literature for the case of neutral, nonretained solutes propelled by electro-osmotic flow. The results further reveal some interesting and somewhat unexpected interactions of the electro-osmotic and Poiseuille components of the elutant flow. Superposition of Poiseuille flow on the natural electro-osmotic flow allows greater freedom in the choice of elutant velocity, without necessarily increasing the dispersion. In fact, it results in lower dispersion under some conditions. Optimum flow conditions are obtained for minimizing the plate height or, equivalently, for maximizing the Peclet number.

Ravindra Datta
Veerabhadra R. Kotamarthi
Department of Chemical and Biochemical Engineering
University of Iowa
Iowa City, IA 52242

Introduction

Capillary electrophoresis (CE), also sometimes called capillary zone electrophoresis (CZE) or high-performance capillary electrophoresis (HPCE), is a new analytical technique that offers the advantages of rapid analysis with excellent resolution of complex biochemical mixtures. The development of CE has generated much excitement since conventional electrophoretic devices are slow and involve manually intensive methodologies. The slow speed in conventional electrophoresis techniques is a result of the traditional use of low electric field strengths ($dV/dz \sim 1$ kV/m), coupled with inherently small values of electrophoretic mobilities ($u_i \sim 10^{-8}$ m^2/V · s) of solutes. Use of high-voltage gradients in electrophoresis has so far been limited by heat transfer considerations since effective heat transfer is crucial to avoid loss of zone resolution because of natural convection, and also the possible denaturation of heat-sensitive, biologically-active compounds. Capillary electrophoresis overcomes this limitation by using very small-diameter capillaries (25–100 μm ID and wall thickness ~200 μm), typically 50–100 cm long, that provide large surface area to volume ratio for effective heat dissipation. This allows the use of extraordinarily high electric fields strengths, of the order of 20–30 kV/m, which results in very efficient separation of complex, closely-related species in a relatively short time period (10–30 minutes). The currents generated are usually less than 200 μA, corresponding to a power dissipation of less than 5 W in the capillary.

The history of the development of CE is described by Compton and Brownlee (1988). Mikkers et al. (1979) first used a 200 μm ID Teflon tube for free-flow electrophoresis with high-voltage drops and obtained efficient separations with unprecedented plate heights of less than 10 μm. Soon thereafter, Jorgenson and Lukacs (1981) utilized 75 μm ID borosilicate glass capillary and successfully separated dansyl amino acids obtaining plate heights of only a few μm. Since then, research on CE has proliferated and the technique has also been extended to other electrophoresis modes such as isotachophoresis, capillary gel electrophoresis, micellar electrokinetic capillary chromatography, and capillary isoelectric focusing. Many reviews have appeared on the subject (e.g., Jorgenson, 1987; Ewing et al., 1989), even though the field is still in its infancy. Tehrani and Day (1989) have provided a summary of the performance characteristics of CE in comparison with conventional gel electrophoresis and high-pressure liquid chromatography.

The most common capillary material now used in CE is fused silica, although glass and Teflon have also been used. The silanol groups on the silica capillary walls acquire a negative charge, with positive counter-ions in the aqueous electrolyte buffer. These hydrated counter-ions are attracted to the cathode and,

Correspondence concerning this paper should be addressed to R. Datta.

therefore, give rise to an electro-osmotic flow toward the cathode. The electro-osmotic flow thus generated can be quite substantial in CE because of the use of high electric field strengths and is, in fact, utilized in CE for the elutant flow instead of the conventional pressure-driven flows. Further, since the electro-osmotic velocity profile is considerably flatter than that in Poiseuille flow, it also results in reduced hydrodynamic dispersion. Unfortunately, however, there is no easy way to control the electro-osmotic flow in an open capillary for a given field strength, apart from capillary surface modifications. This imposes a severe limitation in the choice of elutant velocity which, of course, is easily controlled with conventional pumping in rival analytical techniques such as HPLC.

Another significant advantage of CE as compared with conventional electrophoresis techniques is that, provided a solute does not have strong coulombic or adsorptive interaction with the capillary surface, anionic, cationic and neutral species can be efficiently separated in a single run. The reason for this is that under typical conditions electro-osmotic mobility, u_{eo}, is considerably greater than the electrophoretic mobility, u_i, of most species. Thus, even without the aid of any pressure-driven flow, the electro-osmotic flow generated is sufficiently strong to carry most species, regardless of their charge, toward the cathode. This allows the sample to be introduced at the anode end of the capillary and the separated zones to be detected near the cathode end, with the order of appearance being cationic, neutral and finally anionic species. Separation of protein mixtures with CE has proved to be more difficult, and substantial peak broadening and tailing is encountered. This difficulty arises as a result of the tendency of proteins to adsorb strongly on most capillary surfaces (Lauer and McManigill, 1986). The protein-wall interaction can be substantially reduced by appropriate surface treatment. Substances used for surface modifications include methyl cellulose, polyethylene glycol, and polyacrylamide. However, such surface modifications concomitantly reduce the electro-osmotic flow as well. In such cases, pressure/gravity driven flows may be unavoidable to elute the species. The use of nonaqueous media in CE appears to be promising for some applications and may also require pressure-driven flows.

The objective of this paper is to provide a theoretical model for the electrokinetic dispersion in CE for the general case involving Poiseuille and electro-osmotic elutant flow. The dispersion coefficient is labeled "electrokinetic" to emphasize the combined effects of motion and electrical phenomena. It will be shown that a combination of electro-osmotic and Poiseuille flows not only allows greater freedom in the choice of appropriate elutant velocity, but under certain conditions, can actually provide substantially lower zone spreading. A brief overview of the other causes of zone spreading is provided next before describing the model.

Causes of zone spreading in free-flow electrophoresis

According to Wieme (1975), dispersion in free-flow electrophoresis occurs for the following reasons:

- Axial diffusion is, of course, unavoidable and represents the minimum possible spreading.
- Joule heating, which is generated uniformly throughout the liquid volume but removed only at the capillary surface, results in a radial temperature profile that reduces the fluid viscosity and density in the warmer central parts of the capillary. This also increases the electrophoretic mobility (by about 2% per °C) as well as the electro-osmotic mobility, since both of them are inversely related to the viscosity, as shown in Eqs. 12 and 18, respectively. Thus, the species velocities are higher in the central portion of the capillary, resulting in zone spreading.
- Sample overloading can result in zone spreading and distortion. If the applied sample is concentrated, its conductivity and pH could be quite different from those of the elutant, leading to a local distortion of the electric field and hence resulting in zone spreading.
- Any sorptive interaction of the solute with the capillary surface can substantially contribute to dispersion.
- "Microheterogeneity," i.e., any deviations in size, shape and/or change of the migrating species can cause zone spreading.
- Spreading can also be caused if a migrating species possesses different states that are rapidly interconvertible. This is called "electro-diffusion."
- Gravitational effects, due to any density differences between the fluid and the applied sample, can cause dispersion.
- Elutant flow velocity profile by virtue of laminar flow caused by pressure difference or gravity and/or electro-osmotic flow results in dispersion.

This paper is concerned only with the last factor, the effect of laminar and/or electro-osmotic flow velocity profile on the electrokinetic dispersion. Martin and Guiochon (1984) and Martin et al. (1985) analyzed zone broadening caused by electro-osmotic flow *and* suface adsorption in capillary liquid chromatography. They considered the case of low ζ potential and approximated the electro-osmotic velocity profile by empirical expressions, which were then used in the theory developed by Golay (1958) and Aris (1959) to obtain plate height. They concluded that electro-osmotic flow provides lower zone spreading than pressure-driven flow, but the difference becomes small as the capacity factor of the stationary phase becomes large.

Theoretical Model

Consider a straight cylindrical capillary of diameter d_c and length L shown in Figure 1. The capillary is connected between two reservoirs of an electrolyte buffer, and a constant voltage gradient is applied across it. In addition, a pressure gradient and a gravity component in the axial direction may exist in general. The sample to be separated is introduced as a pulse at $z = 0$. The species migrate at different rates under the influence of the electric field, resulting in separation, and are eluted and detected at $z = L$.

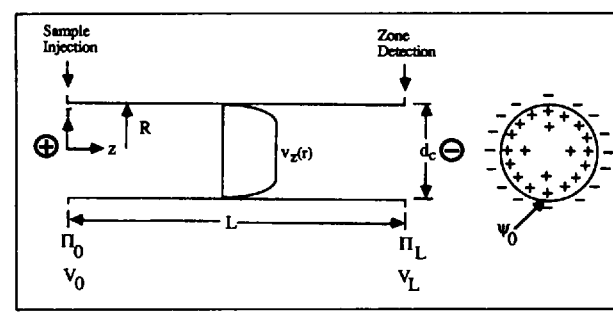

Figure 1. Capillary electrophoresis.

Assumptions

The major assumptions involved in the above analysis are as follows:

1. The capillary is internally isothermal, although the electrolyte temperature may be higher than the ambient temperature.
2. The electrolyte is symmetric: it consists of two types of ions of equal and opposite charge Z, and its properties such as μ, ρ, ϵ, pH, and electrical conductivity are uniform throughout. The solute properties such as u_i and D_i are also constant. Further, the properties of the zones and the elutant are not significantly different.
3. There is no solute adsorption on the capillary surface.
4. The capillary surface has a uniform charge density, and ψ does not vary in the axial direction.
5. The ζ potential is relatively small so that the Debye-Hückel approximation is valid (Probstein, 1989).
6. The L/d_c ratio is large so that the assumptions necessary for a Taylor-type analysis for K_i are valid (Probstein, 1989).
7. There are no perturbations in the elecric field.
8. Other possible causes of zone broadening such as microheterogeneity and electro-diffusion are insignificant.
9. The solute particle size R_p, is much smaller than the capillary size, R, such that effects such as size exclusion are not important (Silebi and DosRamos, 1989).

Formulation

Momentum Balance. The elutant velocity is governed by the Navier-Stokes equation which, in the presence of an electric field, for steady-state, isothermal, one-dimensional, fully-developed flow, takes the form (Probstein, 1989)

$$\mu \frac{1}{r}\frac{d}{dr}\left(r\frac{dv_z}{dr}\right) = \frac{d\Pi}{dz} + \rho_e(r)\frac{dV}{dz}, \tag{1}$$

where $\Pi \equiv p - \pi g_z z$ and accounts for both applied pressure and gravity.

Excess Charge Distribution. The excess charge distribution, $\rho_e(r)$, results from assuming the Boltzmann distribution for the number of ions at a potential ψ above that of the solution (e.g., Gross and Osterle, 1968)

$$\rho_e(r) = -(2Zen)\sinh\left(\frac{Ze\psi}{kT}\right). \tag{2}$$

Poisson's Equation.

$$\frac{1}{r}\frac{d}{dr}\left(r\frac{d\psi}{dr}\right) = -\frac{1}{\epsilon}\rho_e(r). \tag{3}$$

Equations 2 and 3 provide relationships between the excess charge density in electrolyte, ρ_e, and the radial electrostatic potential, ψ.

Species Balance.

$$\frac{\partial C_i}{\partial t} + v_{zi}\frac{\partial C_i}{\partial z} = D_i\left[\frac{1}{r}\frac{\partial}{\partial r}\left(r\frac{\partial C_i}{\partial r}\right) + \frac{\partial^2 C_i}{\partial z^2}\right]. \tag{4}$$

Boundary and Initial Conditions.

$$\text{at} \quad r = 0, \quad \frac{dv_z}{dr} = 0; \quad \frac{d\psi}{dr} = 0; \quad \frac{\partial C_i}{\partial r} = 0. \tag{5}$$

$$\text{at} \quad r = R, \quad v_z = 0; \quad \psi = \psi_0. \tag{6}$$

$$\text{at} \quad t = 0, \quad C_i = \frac{m_i}{\pi R^2}\delta(z). \tag{7}$$

$$\text{at} \quad z \to \pm\infty, \quad C_i = 0, \quad \text{for finite t}. \tag{8}$$

Species velocity

In the above equations, the species velocity, v_{zi}, is the sum of elutant velocity, v_z, and the species electrophoretic velocity, v_{ei}

$$v_{zi} = v_z + v_{ei}, \tag{9}$$

where the electrophoretic velocity of species i is given by

$$v_{ei} = -u_i\frac{dV}{dz}, \tag{10}$$

and is assumed to be uniform throughout the capillary cross section. Although, in the subsequent discussion of this paper, the specific form assumed by an expression for u_i is immaterial, it is useful to briefly discuss it. For a spherical solute particle, balancing the electrical force and the Stokes drag force gives the electrophoretic mobility of species i as

$$u_i = \frac{Q_i^{\pm}}{6\pi\mu R_p}, \tag{11}$$

where u_i assumes positive or negative values depending on the sign of the net species charge, $Q_i^{\pm}$, in which the superscript $\pm$ calls attention to the fact that this quantity is signed. For a simple ion of valency Z_i, $Q_i^{\pm} = Z_i e$; otherwise, $Q_i^{\pm} = \nu_i e$, where ν_i is the *net* number of electronic charges on the particle. Equation 11 is strictly valid only for a spherical particle small enough to be treated as a point charge but large enough for Stokes' equation to apply, and with a thin electric double layer ($\phi_p \to \infty$). In general, the presence of the electric double layer around the particle introduces many additional complexities such as the electrophoretic retardation, surface conductance, and relaxation effects (Probstein, 1989; Wiersema et al., 1966). Accounting for the effect of electrophoretic retardation, which results from the opposite movement of the counter ions in the double layer surrounding the particle and assuming the Debye-Hückel approximation to be valid, Henry's equation results

$$u_i = \frac{2}{3}\frac{\epsilon\zeta_p^{\pm}}{\mu}f(\phi_p), \tag{12}$$

where $\zeta_p^{\pm}$ is signed and the function $f(\phi_p)$ for a spherical particle of radius, R_p, takes the limiting values, $f(\phi_p) \to 1.0$ as $\phi_p \equiv R_p/\lambda \to 0$, and $f(\phi_p) \to 3/2$ as $\phi_p \to \infty$ (Probstein, 1989). A useful relationship between u_i and the diffusion coefficient of solute, D_i, is obtained by comparing Eq. 11 with the Stokes-

Einstein relationship for D_i

$$u_i = \frac{Q_i^{\pm}}{kT} D_i. \tag{13}$$

This relationship has the advantage that it is independent of the shape and size of the solute particle.

Elutant velocity

The excess charge density, ρ_e, can be eliminated between the momentum balance, Eq. 1, and the Poisson's relation, Eq. 3, and the resulting expression integrated subject to the boundary conditions, Eqs. 5 and 6, to yield

$$v_z(y) = v_p(y) + v_e(y), \tag{14}$$

where the Poiseuille velocity profile, as usual, is

$$v_p(y) = \left(-\frac{d\Pi}{dz}\right)\frac{R^2}{4\mu}(1 - y^2), \tag{15}$$

and the electro-osmotic velocity profile is

$$v_e(y) = v_{eo}\left\{1 - \frac{\psi(y)}{\psi_0}\right\}. \tag{16}$$

In this expression, v_{eo} is given by the Helmholtz-Smoluchowski equation

$$v_{eo} = -u_{eo}\frac{dV}{dz}, \tag{17}$$

where the electro-osmotic mobility, u_{eo}, is given by

$$u_{eo} = -\frac{\epsilon\zeta^{\pm}}{\mu}, \tag{18}$$

and is independent of the shape of the capillary. The negative sign in Eq. 18 indicates that, when $\zeta^{\pm}$ is negative, the excess charge in the liquid is positive and, therefore, the electro-osmotic flow is toward the cathode. Note that Eqs. 12 and 18 indicate opposite directions of motion for ζ potential of the same sign.

The area-average elutant velocity may similarly be written in terms of its Poiseuille and electro-osmotic components

$$\langle v_z\rangle = \langle v_p\rangle + \langle v_e\rangle, \tag{19}$$

where

$$\langle v_p\rangle = \left(-\frac{d\Pi}{dz}\right)\frac{R^2}{8\mu}, \tag{20}$$

and

$$\langle v_e\rangle = v_{eo}(1 - \eta). \tag{21}$$

The function η in Eq. 21 is defined by

$$\eta \equiv \frac{2}{\psi_0}\int_0^1 \psi(y) y\, dy. \tag{22}$$

The potential distribution, $\psi(y)$, in Eqs. 16 and 22, is obtained by solving the Poisson-Boltzmann equation resulting from the combination of Eqs. 2 and 3, which in dimensionless form is

$$\frac{1}{y}\frac{d}{dy}\left(y\frac{d\Psi}{dy}\right) = \phi^2 \sinh\Psi. \tag{23}$$

Since this equation cannot be solved analytically, we shall limit our subsequent analysis to the case of relatively low ζ potential ($0 \le \Psi \le 1$) by invoking the Debye-Hückel approximation, which linearizes Eq. 23 by retaining only the first term in the series expansion of $\sinh\Psi$, i.e., $\sinh\Psi \approx \Psi$ (Philip and Wooding, 1970). The solution of the resulting expression is

$$\frac{\psi}{\psi_0} = \frac{I_0(\phi y)}{I_0(\phi)}. \tag{24}$$

In general, Eq. 23 must be solved numerically. For example, Gross and Osterle (1968) have provided a plot of Ψ vs. dimensionless radial distance in the capillary, y, for the case of $\Psi_0 = 2.79$, and for different values of ϕ. While we plan to treat the nonlinear case of arbitrary ζ potential in subsequent work, it is of interest to point out here that the computational results of Gross and Osterle are not very different from those predicted by Eq. 24. Nonetheless, when Eq. 24 is used in Eqs. 16 and 21 the electro-osmotic velocity profile takes the form (Rice and Whitehead, 1965)

$$v_e = v_{eo}\left\{1 - \frac{I_0(\phi y)}{I_0(\phi)}\right\}. \tag{25}$$

Further, using Eq. 24 in Eq. 22

$$\eta = \frac{2}{\phi}\frac{I_1(\phi)}{I_0(\phi)}. \tag{26}$$

Equation 26 is of the familiar form of the so-called effectiveness factor for first-order reaction in a cylindrical catalyst particle and has the limiting forms: $\eta \to 1.0$ as $\phi \to 0$ and $\eta \to 2/\phi$ as $\phi \to \infty$. The electro-osmotic velocity profile described by Eq. 25 is plotted in a dimensionless form in Figure 2. For small capillaries described by the dimensionless capillary radius $\phi = 3$ in the figure, the velocity profile qualitatively resembles Poiseuille velocity profile. For large capillaries, however, when the capillary radius is much larger than the Debye length, λ, the cases corresponding to $\phi \ge 10$ in the figure, the velocity profile is substantially flat over a major portion of the capillary cross section. The area-average electro-osmotic flow velocity given by Eq. 21 is plotted in a dimensionless form in Figure 3 as a function of the dimensionless capillary radius, ϕ. It is seen that as $\phi \to \infty$, $\langle v_e\rangle \to v_{eo}$. Finally, the reduced total elutant velocity profile for the general case when both the Poiseuille and electro-osmotic flows coexist, as given by Eq. 27 below obtained by combining Eqs. 14 to 25, is plotted in Figure 4.

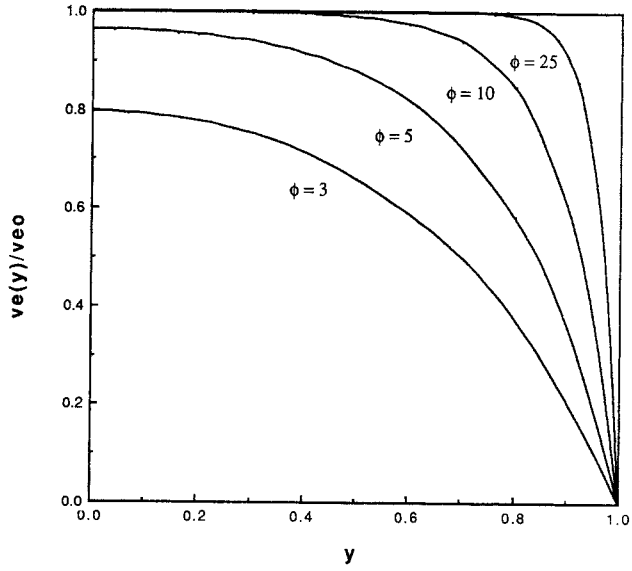

Figure 2. Dimensionless electro-osmotic velocity profile for different dimensionless capillary radii, ϕ.

$$\frac{v_z(y)}{\langle v_z\rangle} = 2\nu(1-y^2) + \frac{1-\nu}{1-\eta}\left\{1 - \frac{I_0(\phi y)}{I_0(\phi)}\right\}. \qquad (27)$$

Here ν is defined as the fraction of the total elutant flow caused by Poiseuille flow,

$$\nu \equiv \frac{\langle v_p\rangle}{\langle v_z\rangle}. \qquad (28)$$

It should be noted here that the parameter ν is not necessarily limited to values between 0 and 1, but can, in theory, vary from $-\infty$ to $+\infty$, or more restrictively, within limits of laminar flow.

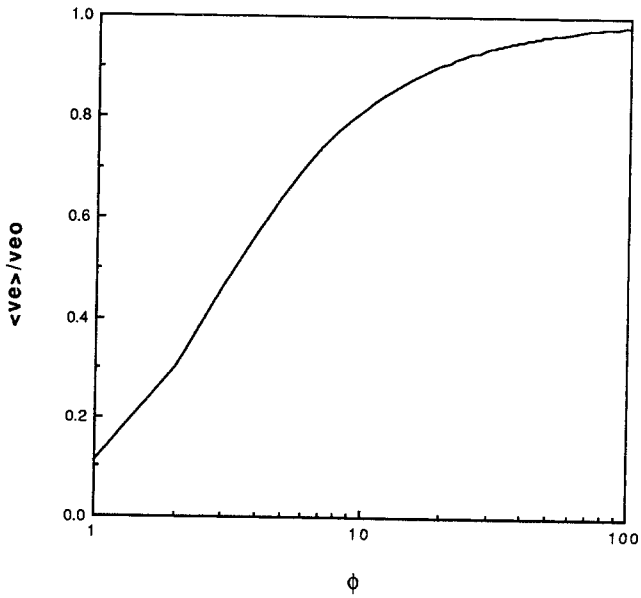

Figure 3. Dimensionless area-average electro-osmotic velocity vs. dimensionless capillary radius, ϕ.

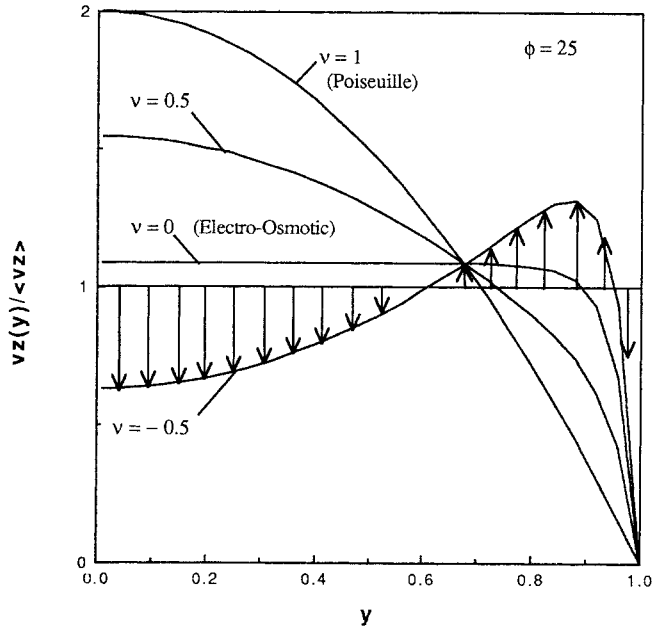

Figure 4. Reduced total velocity profile for different Poiseuille flow fractions of elutant flow, ν, for a dimensionless capillary radius, $\phi = 25$.

Figure 4 provides a comparison of the elutant velocity profiles for the four cases of ν: $\nu = -0.5$, 0, 0.5, and 1.0 when $\phi = 25$. The case of $\nu = 1.0$ corresponds to the familiar parabolic form of Poiseuille flow only, and $\nu = 0$ corresponds to the case of electro-osmotic flow only, being considerably flatter for this relatively large capillary size. $\nu = 0.5$ corresponds to the case of half the elutant flow contributed by Poiseuille flow, whereas $\nu = -0.5$ refers to the case when Poiseuille flow opposes the elutant flow. It is useful at this time to examine the deviation of the flow profiles from the mean velocity for these various cases, and the particular case of $\nu = -0.5$ is highlighted by arrows, since it is this velocity deviation that gives rise to the dispersion coefficient, K_i, to be considered shortly.

Concentration profile

The area-average concentration profile of solute, i, is of the primary interest. For this purpose, the species balance equation, Eq. 4, is first area-averaged to obtain the so-called Taylor dispersion equation (Probstein, 1989)

$$\frac{\partial\langle C_i\rangle}{\partial t} + \langle v_{zi}\rangle\frac{\partial\langle C_i\rangle}{\partial z} = K_i\frac{\partial^2\langle C_i\rangle}{\partial z^2}, \qquad (29)$$

where K_i is obtained as described in the next section. The area-averaged species velocity, $\langle v_{zi}\rangle$, from Eq. 9 is

$$\langle v_{zi}\rangle = \langle v_z\rangle + v_{ei}, \qquad (30)$$

where $\langle v_z\rangle$ is given by Eq. 19. The solution to Eq. 29, subject to Eqs. 7 and 8, predicts Gaussian concentration profile for i

$$\langle C_i\rangle = \frac{\dfrac{m_i}{\pi R^2}}{\sqrt{4\pi K_i t}}\exp\left(-\frac{z_1^2}{4K_i t}\right), \qquad (31)$$

where z_1 represents the axial distance from the plane moving with the average species velocity,

$$z_1 = z - \langle v_{zi} \rangle t. \tag{32}$$

Electrokinetic dispersion coefficient, K_i

The approach originally developed by Westhaver (1947), and later more elegantly by Taylor (1953) and in greater generality by Aris (1956), is followed to obtain an expression for the dispersion coefficient, K_i. This approach yields

$$K_i = D_i - \frac{2R^2}{D_i} \int_0^1 \Delta C_i'(y) \Delta v_{zi}(y) y \, dy, \tag{33}$$

where the function

$$\Delta C_i'(y) \equiv \int_0^y \frac{1}{y'} \left\{ \int_0^{y'} \Delta v_{zi}(y'') y'' dy'' \right\} dy', \tag{34}$$

and Δv_{zi} is the radial species velocity deviation with respect to $\langle v_{zi} \rangle$

$$\Delta v_{zi}(y) \equiv v_{zi}(y) - \langle v_{zi} \rangle. \tag{35}$$

Using Eqs. 9, 14 to 25 and Eq. 30 in Eq. 35 gives

$$\Delta v_{zi}(y) = \langle v_p \rangle (1 - 2y^2) + \langle v_e \rangle \cdot \left\{ \frac{\eta}{1 - \eta} - \frac{1}{1 - \eta} \frac{I_0(\phi y)}{I_0(\phi)} \right\}. \tag{36}$$

The integration indicated in Eqs. 33 and 34 is straightforward, although somewhat tedious, and involves Lommel's integral (Tranter, 1968). The final result is

$$K_i = D_i + \frac{X_p R^2}{D_i} \{ \langle v_p \rangle^2 + \delta_2 \langle v_p \rangle \langle v_e \rangle + \delta_3 \langle v_e \rangle^2 \}, \tag{37}$$

where

$$\delta_2 = \frac{X_{pe}}{X_p}, \tag{38}$$

$$\delta_3 = \frac{X_e}{X_p}, \tag{39}$$

and the functions

$$X_p = \frac{1}{48}, \tag{40}$$

$$X_{pe} = \frac{\eta}{1 - \eta} \left\{ \frac{1}{12} - \frac{2}{\phi^2} + \frac{16}{\phi^4} \left(\frac{1 - \eta}{\eta} \right) \right\}, \tag{41}$$

and

$$X_e = \frac{\eta^2}{(1 - \eta)^2} \left\{ \frac{3}{8} + \frac{2}{\phi^2} - \frac{1}{\eta \phi^2} - \frac{1}{\eta^2 \phi^2} \right\}. \tag{42}$$

In these expressions, η is given by Eq. 26 and is a function of ϕ only. Therefore, δ_2 and δ_3 are functions only of the dimensionless capillary radius, ϕ, and are plotted in Figure 5. It is seen that both δ_2 and δ_3 are of the order of unity for small ϕ and decrease as ϕ increases, δ_3 more so than δ_2. Actually, δ_2 initially increases with ϕ at small ϕ. For relatively large ϕ, the limiting form $\eta \approx 2/\phi$ may be used in the equations for δ_2 and δ_3.

Equation 37 gives K_i in terms of the area-average Poiseuille and electro-osmotic flow velocities, $\langle v_p \rangle$ and $\langle v_e \rangle$, but is independent of the electrophoretic migration velocity of i, v_{ei}, since this was assumed to be independent of the radial coordinate. The functional dependence of K_i on $\langle v_p \rangle$ and $\langle v_e \rangle$ is quite interesting and not of a form that was intuitively obvious to the authors. Since $\langle v_p \rangle$ or $\langle v_e \rangle$ may assume negative values as well, the second term in the braces of Eq. 37 will then become negative and can cause the dispersion coefficient to become smaller. Note that when there is no electro-osmotic flow, $\langle v_e \rangle = 0$, Eq. 37 reduces to the familiar expression for laminar flow (Westhaver, 1947; Aris, 1956)

$$K_{i0} = D_i + \frac{R^2}{48 D_i} \langle v_p \rangle^2. \tag{43}$$

In the case of electro-osmotic flow only, for $\langle v_p \rangle = 0$, the dispersion coefficient is

$$K_i = D_i + \frac{R^2}{48 D_i} \delta_3 \langle v_e \rangle^2. \tag{44}$$

Dimensionless forms for K_i

It is convenient, for the purpose of further discussion, to cast Eq. 37 into dimensionless forms. Thus

$$\frac{K_i}{D_i} = 1 + \frac{X_p}{4} (ReSc)^2 \{ \nu^2 + \delta_2 \nu (1 - \nu) + \delta_3 (1 - \nu)^2 \}, \tag{45}$$

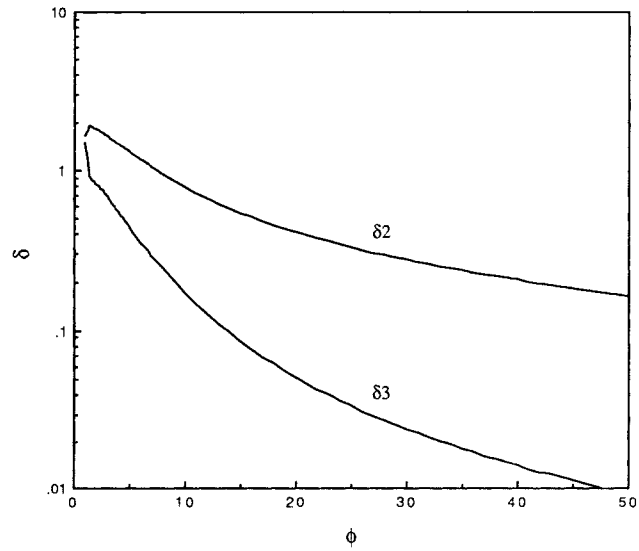

Figure 5. Functions δ_2 and δ_3 as a function of the dimensionless capillary radius, ϕ.

where the product of the Reynold and Schmidt numbers is

$$ReSc = \frac{d_c\langle v_z\rangle}{D_i}, \tag{46}$$

which is frequently also called the (molecular) diffusion Peclet number, Pe_D, in the dispersion literature. Note that this is distinct from the Peclet number, Pe, as defined below in Eq. 47, which has K_i in the denominator rather than D_i. In order to avoid confusion, we will call the dimensionless quantity in Eq. 46 as the product $ReSc$ rather than Pe_D. It should also be noted that in defining Pe_D the characteristic dimension R has often been used in the literature in place of capillary diameter, d_c, used here. In Eq. 45, ν is defined by Eq. 28 and is the ratio of the Poiseuille velocity $\langle v_p\rangle$ to the total elutant velocity, $\langle v_z\rangle$.

Another useful dimensionless form of Eq. 37 is in terms of Peclet number, Pe, or the height equivalent of a theoretical plate (HETP) for *neutral* ($u_i = 0$) solutes, H, defined by

$$Pe \equiv \frac{d_c\langle v_z\rangle}{K_i}, \tag{47}$$

and

$$H \equiv \frac{2K_i}{\langle v_z\rangle}. \tag{48}$$

Then

$$\frac{H}{2d_c} = \frac{1}{Pe} = \frac{1}{ReSc} + \frac{X_p}{4}(ReSc) \cdot \{\nu^2 + \delta_2\nu(1-\nu) + \delta_3(1-\nu)^2\}. \tag{49}$$

The plate height for neutral solutes, H, given by the above equation is, like K_i, seen to be independent of the electrophoretic velocity of the migrating species, v_{ei}. In general, however, this would not be true, since the plate height is, in general, defined by $H_i = 2K_i/\langle v_{zi}\rangle$, and, therefore, would depend upon the magnitude as well as the sign of v_{ei}.

Discussion of Results

Comparison with experiments for electro-osmotic flow

Some data on electrokinetic dispersion are available in the literature for the case of electro-osmotic flow only, i.e., for $\nu = 0$. The first systematic study was conducted by Pretorius et al. (1974), who investigated the proposed use of electro-osmotic flow of elutant in HPLC instead of the conventional high-pressure pump, in an effort to reduce zone spreading. They measured the plate heights at different electro-osmotic flow rates by varying the voltage gradients in capillaries as well as in packed beds. Their data for a quartz tube of radius 0.05 cm for the uncharged solute, benzene, in methanol as an elutant is presented in Figure 6, along with a comparison provided by Eq. 49 for both the cases of only Poiseuille flow ($\nu = 1$) and for only electro-osmotic flow ($\nu = 0$). The value of the diffusion coefficient, $D_i = 1 \times 10^{-5}$ cm^2/s, was assumed to be the same as suggested by Pretorius et al. For the case of $\nu = 0$, $\phi = 25$ was used as the fitted parameter which provides an excellent fit

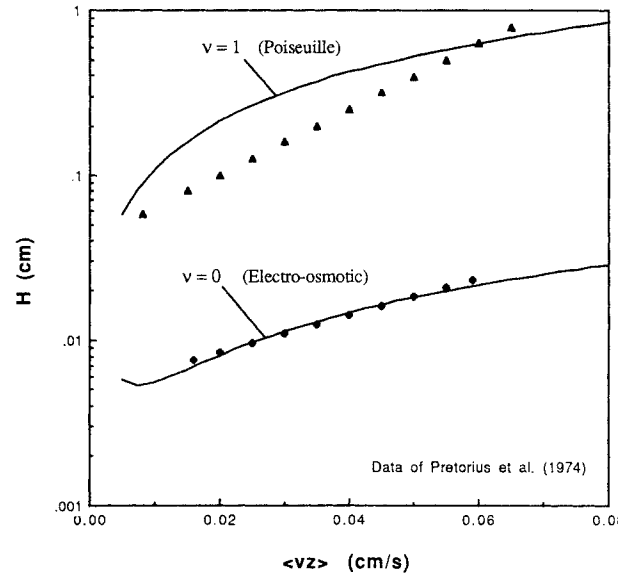

Figure 6. Theory vs. experimental results of Pretorius *et al.* (1974): plate height for the unretained solute benzene with methanol as an elutant in a quartz capillary of radius 0.05 cm.

$\phi = 25$ is used as a fitted parameter.

between the theory and experiments. This would imply a double layer thickness, $\lambda = 20$ μm. While this may appear as a large value, Martin and Guiochon (1984) also obtained this value in their numerical simulation of the data. It may, therefore, be concluded that the derived expression is correct. It should also be noted from Figure 6 that the HETP values obtained for electro-osmotic flow are an order of magnitude lower than those for laminar flow.

Tsuda et al. (1982) also measured HETP values in liquid chromatography as a function of electro-osmotic flow velocity in a Pyrex capillary tube of radius 61 μm. They used pyridine as the nonretained solute which is neutral in the buffer used, Na_2HPO_4-H_2O. Figure 7 provides a comparison of their experimental results with our model predictions. The value of $D_i = 9.2 \times 10^{-6}$ cm^2/s suggested by Tsuda et al. was employed and $\phi = 33$ ($\lambda = 1.8$ μm) was used as the fitted parameter. This ϕ agrees well with the value obtained by Martin and Guiochon (1984) in their numerical simulation of the data.

In capillary electrophoresis, similar careful data have not been reported in the literature so far, although separation efficiency in terms of number of theoretical plates, N, as a function of applied voltage has been reported by Jorgenson and Lukacs (1981). N given is of the order of 2.5×10^5 theoretical plates. It is commonly assumed in the CE literature that the electro-osmotic flow is completely flat and, therefore, diffusion is the only cause of zone spreading. This is, obviously, incorrect.

Further implications of results

It is customarily assumed that electro-osmotic flow is adequate in CE and, in fact, pressure or gravity-driven elutant flow is considered undesirable due to the perception that it would cause increased zone spreading. This issue is investigated next in some detail. It has been mentioned before that the superposition

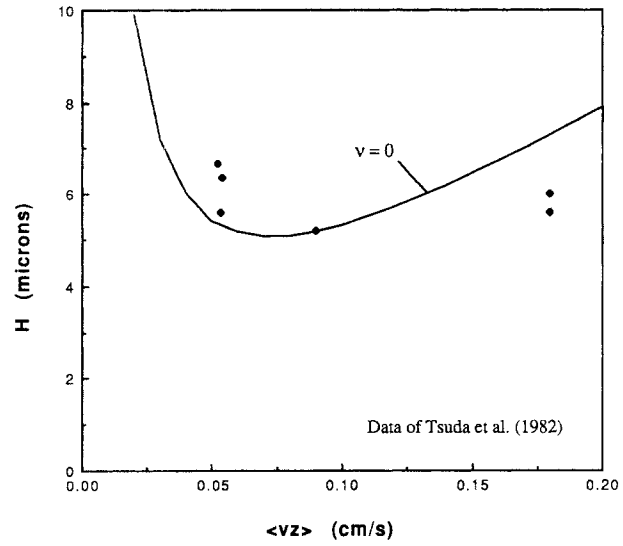

Figure 7. Theory vs. experimental results of Tsuda *et al.* (1982): plate height for the unretained solute pyridine with Na_2HPO_4-H_2O as an elutant in a Pyrex capillary of radius 61 μm.

$\phi = 33$ is used as a fitted parameter.

of pressure-driven flow on electro-osmotic flow provides an additional degree of freedom in CE, and, in fact, some hydrostatic pressure may be unavoidable in practical CE systems unless great care is exercised to ensure a completely open capillary. It will be shown that under certain conditions, with a judicious combination of pressure-driven and electro-osmotic flows, in fact a reduction in dispersion coefficient may be obtained.

Equation 45 is plotted in Figure 8 as K_i/D_i vs. $ReSc$ (or Pe_D) for a variety of ν values. It should be noted that for aqueous elutants, Schmidt number is of the order of 1,000 and is a constant. Thus, variation in $ReSc$ merely reflects variation in the elutant velocity. A dimensionless capillary radius $\phi = 25$ is utilized in Figure 8, since this appears to be a typical value from our discussion of previous literature data. At small $ReSc$, the second term on the righthand side of Eq. 45 $\rightarrow 0$, and, therefore, all the curves in Figure 8 tend to come to unity. Further, as $ReSc \rightarrow \infty$, the second term on the righthand side of Eq. 45 becomes much larger than unity, thus first item may be dropped. Thus, at large $ReSc$, the slope of all curves on a plot of log (Ki/Di) vs. log $(ReSc)$ becomes constant and equals 2.

Figure 8 has other interesting features. First, as expected, K_i for electro-osmotic flow only ($\nu = 0$) is substantially smaller than that for pressure-driven flow only ($\nu = 1$). As may also be expected, when $\nu = 0.5$, corresponding to half-presure-driven and half-electro-osmotic flow, K_i assumes values that are intermediate between $\nu = 1$ and $\nu = 0$. When $\nu > 1$, in which case electro-osmotic flow opposes elutant bulk flow, K_i is seen to be greater than that for pressure-driven flow only ($\nu = 1$). However, the case of $\nu < 0$, in which pressure-driven flow opposes bulk elutant flow, it is particularly interesting. For $\nu = -0.5$, values of K_i are obtained that are less than those for $\nu = 0.5$ but higher than those for electro-osmotic flow only ($\nu = 0$). However, for $\nu = -0.2$, values of K_i are substantially lower than even the case of only electro-osmotic flow are obtained. This fact becomes more obvious in Figure 9, in which K_i as a ratio of K_{i0}, the dispersion coefficient for pressure-driven flow alone given by Eq. 43 is plotted vs. $ReSc$. It is obvious that a judicious choice of ν could reduce K_i. The asymptotic behavior of Eq. 45 for large $ReSc$ is also obvious in Figure 9 and causes $K_i/K_{i0} \rightarrow$ constant as $ReSc \rightarrow \infty$.

Figure 10 shows a plot of K_i/K_{i0} vs. ν for $\phi = 25$ and $ReSc = 250$. It is seen that this curve goes through a minimum for $\nu \approx -0.2$. For large ν, negative or positive, K_i can be substantially greater than K_{i0}, and there is a minimum at an intermediate value. This optimum ν, ν_o, may be obtained by differentiating

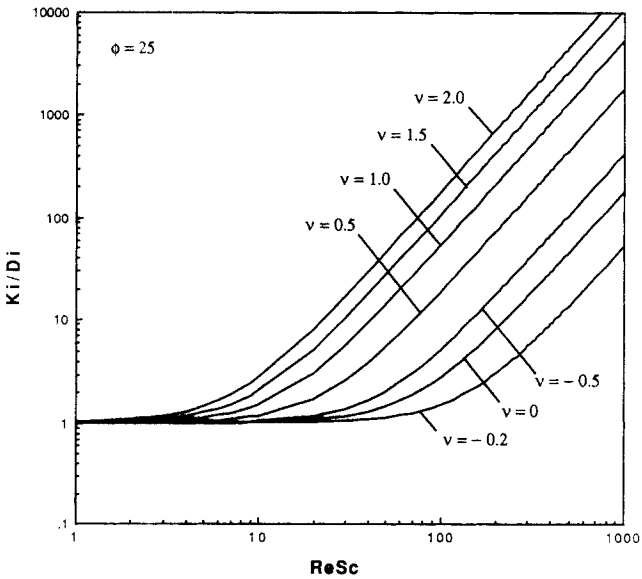

Figure 8. K_i/D_i vs. $ReSc$ (or Pe_D) for $\phi = 25$ and for a variety of ν values.

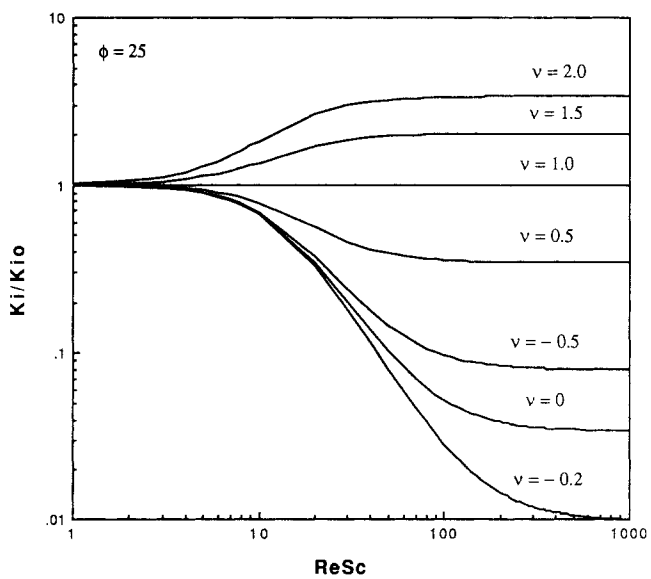

Figure 9. K_i/K_{i0} vs. $ReSc$ (or Pe_D) for $\phi = 25$ and for a variety of ν values.

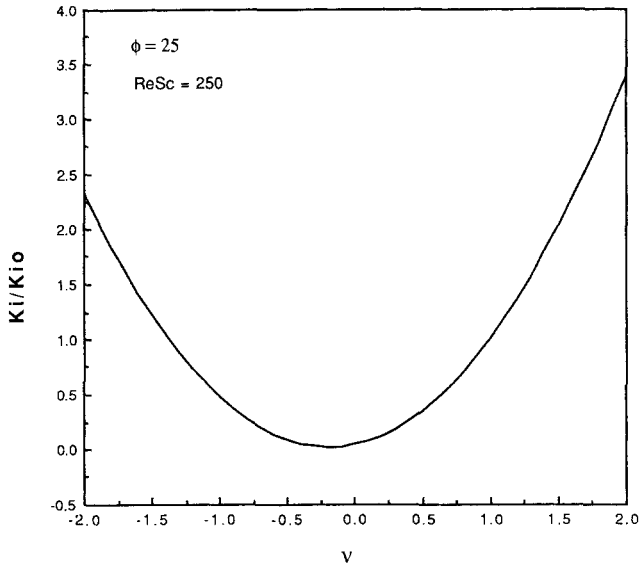

Figure 10. K_i/K_{io} vs. ν for $\phi = 25$ and for $ReSc$ (or Pe_D) = 250.

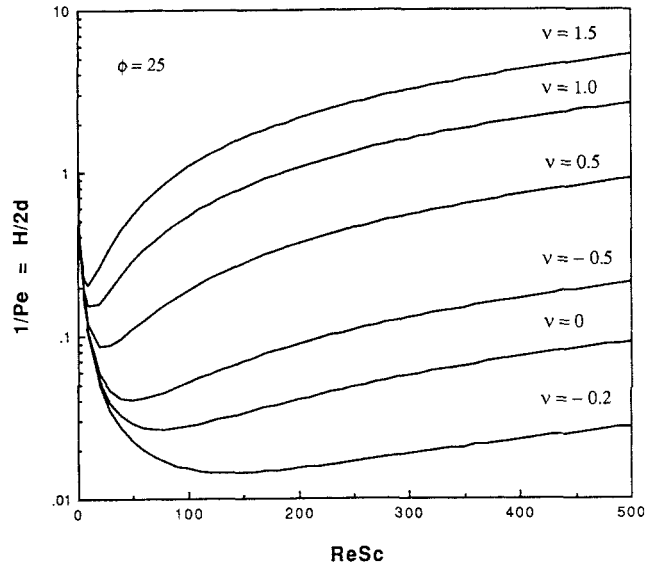

Figure 12. Dimensionless plate height for a neutral solute vs. $ReSc$ (or Pe_D) for $\phi = 25$ and for a variety of ν values.

Eq. 45 and setting $\partial K_i/\partial \nu = 0$. This yields

$$\nu_o = \frac{\delta_2 - 2\delta_3}{2(\delta_2 - \delta_3 - 1)}. \tag{50}$$

It should be noted that ν_o is a function of ϕ only. Equation 50 is plotted in Figure 11 to provide ν_o vs. ϕ. It is seen that ν_o is always negative and $\nu_o \to 0$ as $\phi \to \infty$. Equation 50 could alternately be obtained by differentiating Eq. 49 and setting $\partial(1/Pe)/\partial\nu = 0$. Therefore, ν_o also corresponds to a minimum in H or $1/Pe$ with respect to the parameter ν.

Equation 49 is plotted in Figure 12 to provide dimensionless plate height for neutral solutes vs. $ReSc$ for a variety of ν values. Such plots would be useful in determining the optimum elutant velocity in order to minimize HETP in CE. First, it may be noted that the relative variation of H with ν is qualitatively similar to that of K_i. Secondly, H goes through a minimum with $ReSc$, the location of which depends upon the value of ν. It is seen that for $\nu = -0.2$, not only is this minimum lower than that for $\nu = 0$, but the subsequent slope of the curve is also smaller. This has important practical implications, since, for the purpose of speedy analysis, it is frquently desirable to operate at an elutant velocity higher than that corresponding to the minimum in H. At any rate, the optimum $ReSc$, $(ReSc)_o$, can be obtained by differentiating Eq. 49 and setting $\partial(1/Pe)/\partial(ReSc) = 0$, resulting in

$$(ReSc)_o = 2[X_p\{\nu^2 + \delta_2\nu(1 - \nu) + \delta_3(1 - \nu)^2\}]^{-1/2} \tag{51}$$

which is a function of ϕ and ν only. Figure 13 shows a plot of Eq. 51 for $(ReSc)_o$ vs. ν for $\phi = 25$. For a given capillary size, global optimum $ReSc$ can be obtained by utilizing $\nu = \nu_o$ predicted in Eq. 50 in Eq. 51. Note the sharp maximum in $(ReSc)_o$ at $\nu = \nu_o$ in Figure 13.

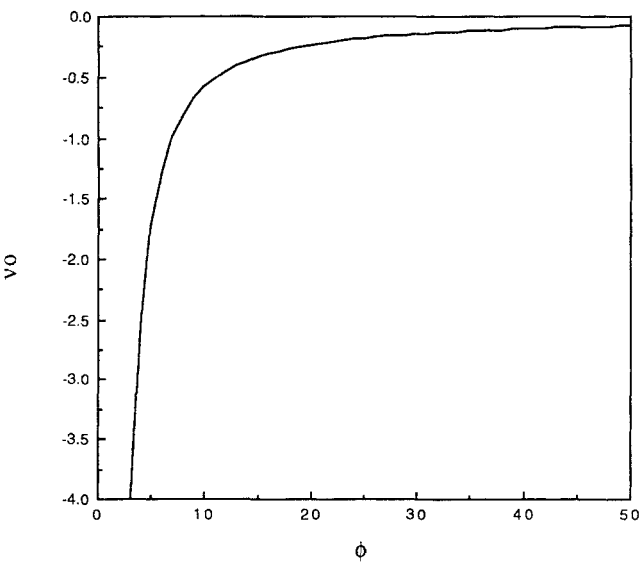

Figure 11. Optimum Poiseuille flow fraction of the elutant flow, ν_o, as a function of the dimensionless capillary radius, ϕ.

Conclusion

In this paper, we derived an analytical expression for the electrokinetic dispersion coefficient, K_i, in capillary electrophoresis for the case of low ζ potential that accounts for the combined effects of electro-osmotic and hydrodynamic flows. The nonlinear general case involving arbitrary ζ potential is planned to be treated subsequently. There is good agreement between the model and experimental results for HETP values reported in the literature for the case of electro-osmotic flow, provided that the double-layer thickness, λ, is used as a fitted parameter. The values of λ thus assumed, however, agree with those obtained by Martin and Guiochon (1984) in their numerical simulation.

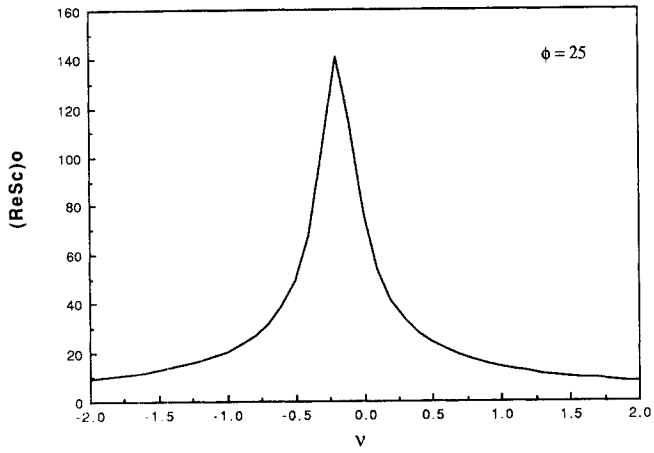

Figure 13. Optimum *ReSc* (or Pe_D), $(ReSc)_o$, for $\phi = 25$ as a function of ν.

The results show that the presence of pressure-driven flow, while allowing greater operational freedom, is not always deleterious to the CE performance. In fact, under certain conditions, the electrokinetic dispersion coefficient can be further reduced in the presence of a small, negative, pressure-driven flow. At any rate, the presence of a small hydrodynamic flow component does not substantially alter K_i, while offering some freedom in the choice of elutant flow rates for best performance. Optimum conditions are provided for minimizing HETP.

Acknowledgment

The authors would like to thank Janusz Gorowicz, Randall Yoshisato, Gregory Carmichael and Robert Beardsley for their contributions through many discussions on this and related topics.

Notation

C_i = concentration of species i, mol · m^{-3}
$\langle C_i \rangle$ = cross-sectional area-averaged concentration of i, mol · m^{-3}
ΔC_i = radial concentration deviation from that at the capillary axis, mol · m^{-3}
$\Delta C_i'$ = function defined by Eq. 34, $\Delta C_i' = D_i \Delta C_i / R^2 (\partial \langle C_i \rangle / \partial z_1)$, m · s^{-1}
D_i = diffusion coefficient of solute i in liquid elutant, m^2 · s^{-1}
d_c = capillary internal diameter, m
e = charge on an electron/proton = 1.60210×10^{-19} C
g_z = z component of the acceleration due to gravity, m · s^{-2}
H = height equivalent of a theoretical plate for a neutral solute, Eq. 48, m
H_i = height equilvalent of a theoretical plate for a (charged) solute = $2K_i / \langle v_{zi} \rangle$, m
K_i = electrokinetic dispersion coefficient of species i, m^2 · s^{-1}
K_{i0} = electrokinetic dispersion coefficient for Poiseuille flow only, m^2 · s^{-1}
k = Boltzmann constant, 1.38054×10^{-23} J · K^{-1}
L = capillary length, m
m_i = total moles of species i fed, mol
N = number of theoretical plates = L/H
n = number of positive/negative electrolyte ions per unit volume, m^{-3}
p = pressure, Pa
Pe = Peclet number = $d_c \langle v_z \rangle / K_i$, dimensionless
Pe_D = molecular diffusion Peclet number = $d_c \langle v_z \rangle / D_i$ = $ReSc$, dimensionless
$Q_i^{\pm}$ = net charge on each particle of species i, = $\nu_i e$, C
R = capillary radius, m
Re = Reynold number ≡ $d_c \langle v_z \rangle \rho / \mu$, dimensionless
R_p = effective particle radius, m
r = radial coordinate
Sc = Schmidt number ≡ $\mu / \rho D_i$, dimensionless
t = time, s
u_{eo} = electro-osmotic mobility of elutant, Eq. 18, m^2 · V^{-1} · s^{-1}
u_i = electrophoretic mobility of species i, m^2 · V^{-1} · s^{-1}
V = electric potential, V
v_e = electro-osmotic flow velocity of elutant, m · s^{-1}
v_{eo} = maximum possible electro-osmotic velocity, Eq. 17, m · s^{-1}
$\langle v_e \rangle$ = cross-sectional area-averaged electro-osmotic velocity, m · s^{-1}
v_{ei} = electrophoretic velocity of species i, Eq. 10, m · s^{-1}
v_p = Poiseuille velocity, due to pressure difference or gravity, Eq. 15, m · s^{-1}
$\langle v_p \rangle$ = cross-sectional area-averged Poiseuille velocity, Eq. 20, m · s^{-1}
v_z = axial elutant velocity, Eq. 14, m · s^{-1}
$\langle v_z \rangle$ = cross-section area-averaged elutant velocity, Eq. 19, m · s^{-1}
v_{zi} = total axial velocity of species i, Eq. 9, m · s^{-1}
$\langle v_{zi} \rangle$ = cross-section area-averaged and velocity of specis i, Eq. 30, m · s^{-1}
y = dimensionless radial coordinate = r/R
y' = dummy variable of integration in Eq. 34
y'' = dummy variable of integration in Eq. 34
Z = charge number of the symmetric electrolyte buffer
Z_i valency of a simple ion i
z = axial coordinate, m
z_1 = axial distance with respect to a plane moving with a velocity $\langle v_{zi} \rangle$, m

Greek letters

δ_2 = function defined by Eq. 38, dimensionless
δ_3 = function defiined by Eq. 39, dimensionless
$\delta(z)$ = impulse function
ϵ = permittivity of elutant = $\epsilon_r \epsilon_0$, C · V^{-1} · m^{-1}
ϵ_r = relative permittivity, dimensionless
ϵ_0 = permittivity of vacuum = 8.854×10^{-12} C · V^{-1} · m^{-1}
$\zeta^{\pm}$ = zeta potential of capillary surface (at the plane of shear), V
$\zeta_p^{\pm}$ = zeta potential of particle surface, V
η = function of ϕ, Eqs. 22 and 26
λ = Debye length = $\sqrt{\epsilon k T / 2n(Ze)^2}$, m
μ = elutant viscosity, Pa · s
ν = the Poiseuille velocity ratio of elutant, $\langle v_p \rangle / \langle v_z \rangle$
ν_i = the net number of electronic charges on the solute particle
Π = combined applied and hydrostatic pressure = $p - \rho g_z z$, Pa
ρ = elutant density, kg · m^{-3}
ρ_e = excess electric charge density in liquid, C · m^{-3}
ϕ = dimensionless capillary radius = R/λ
ϕ_p = dimensionless particle radius = R_p/λ
X_e = function defined by Eq. 42, dimensionless
X_p = function defined by Eq. 40, dimensionless
X_{pe} = function defined by Eq. 41, dimensionless
Ψ = dimensionless electrostatic potential = $Ze\psi/kT$
Ψ_0 = dimensionless electrostatic potential at capillary surface at $r = R$, = $Ze\psi_0/kT$
ψ = electrostatic potential in elutant due to excess charge, V
ψ_0 = electrostatic potential in elutant at the capillary surface at $r = R$, V

Literature Cited

Aris, R., "On the Dispersion of a Solute in a Fluid Flowing through a Tube," *Proc. Roy. Soc., Lond.*, **A 235,** 67 (1956).

———, "On the Dispersion of a Solute by Diffusion, Convection and Exchange between Phases," *Proc. Roy. Soc., Lond.*, **A 252,** 538 (1959).

Compton, S. W., and R. G. Brownlee, "Capillary Electrophoresis," *BioTechniques*, **6**(5), 432 (1988).

Ewing, A. G., R. A. Wallingford, and T.M. Olefirowicz, "Capillary Electrophoresis," *Anal. Chem.*, **61,** 292A (1989).

Golay, M. J. E., "Theory of Chromatography in Open and Coated Tubular Columns with Round and Rectangular Cross-sections," D. H. Desty, ed., *Gas Chromatography*, 36, Butterworths, London (1958).

Gross, R. J., and J. F. Osterle, "Membrane Transport Characteristics of Ultrafine Capillaries," *J. Chem. Phys.*, **49,** 228 (1968).
Jorgenson, J. W., "Capillary Zone Electrophoresis," J. W. Jorgenson and M. Phillips, eds., *New Directions in Electrophoretic Methods, ACS Symp. Ser.*, 335, Washington, DC (1987).
Jorgenson, J. W., and K. D. Lukacs, "Zone Electrophoresis in Open-Tubular Glass Capillaries," *Anal. Chem.*, **53,** 1298 (1981).
Lauer, H. H., and D. McManigill, "Capillary Zone Electrophoresis of Proteins in Untreated Fused Silica Tubing," *Anal. Chem.*, **58,** 166 (1986).
Martin, M. and G. Guiochon, "Axial Dispersion in Open-Tubular Capillary Liquid Chromatography with Electro-osmotic Flow," *Anal. Chem.*, **56,** 614 (1984).
Martin, M., and G. Guiochon, Y. Walbroehl, and J. W. Jorgenson, "Peak Broadening in Open-Tubular Liquid Chromatography with Electro-osmotic Flow," *Anal. Chem.*, **57,** 559 (1985).
Mikkers, F. E. P., F. M. Everaerts, Th. P. E. M. Verheggan, "High-Performance Zone Electrophoresis," *J. Chromatog.*, **169,** 11 (1979).
Philip, J. R., and R. A. Wooding, "Solution of the Poisson-Boltzmann Equation About a Cylindrical Particle," *J. Chem. Phys.*, **52,** 953 (1970).
Pretorius, V., B. J. Hopkins, and J. D. Schieke, "Electro-osmosis: A New Concept for High-Speed Liquid Chromatography," *J. Chromatog.*, **99,** 23 (1974).
Probstein, R. F., *Physicochemical Hydrodynamics. An Introduction,* Butterworths, Boston (1989).
Rice, C. L., and R. Whitehead, "Electrokinetic Flow in a Narrow Cylindrical Capillary." *J. Phys. Chem.*, **69,** 4017 (1965).
Silebi, C. A., and J. G. DosRamos, "Axial Dispersion of Submicron Particles in Capillary Hydrodynamic Fractionation," *AIChE J.*, 1351 (1989).
Taylor, G. I., "Dispersion of Soluble Matter in Solvent Flowing Slowly through a Tube," *Proc. Roy. Soc., Lond.*, **A 219,** 186 (1953).
Tehrani, J., and L. Day, "High Performance Capillary Electrophoresis Using a Modular System," *Amer. Biotech. Lab.*, 32 (Nov.–Dec., 1989).
Tranter, C. J., *Bessel Functions With Some Physical Applications,* Hart Pub. Co., New York (1968).
Tsuda, T., K. Nomura, and G. Nakagowa, "Open-tubular Microcapillary Liquid Chromatography with Electro-Osmosis Flow using a UV Detector," *J. Chromatog.*, **248,** 241 (1982).
Westhaver, J. W., "Concentration of Potassium^{39} by Countercurrent Electro-migration: Some Theoretical Aspects of the Operation," *J. Res. Nat. Bur. Standards,* **38,** 169 (1947).
Wieme, R. J., "Theory of Electrophoresis," E. Heftmann, ed., *Chromatography: A Laboratory Handbook of Chromatographic and Electrophoretic Methods,* 3rd ed. (1975).
Wiersema, P. H., A. L. Loeb, and J. Th. G. Overbeek, "Calculation of the Electrophoretic Mobility of a Spherical Colloid Particle," *J. Colloid Interf. Sci.*, **22,** 78 (1966).

Manuscript received Jan. 4, 1990, and revision Apr. 18, 1990.